Cell Reports, Volume *19*

Supplemental Information

Locally Triggered Release of the Chemokine CCL21 Promotes Dendritic Cell Transmigration across Lymphatic Endothelia

Kari Vaahtomeri, Markus Brown, Robert Hauschild, Ingrid De Vries, Alexander Franz Leithner, Matthias Mehling, Walter Anton Kaufmann, and Michael Sixt

Figure S1

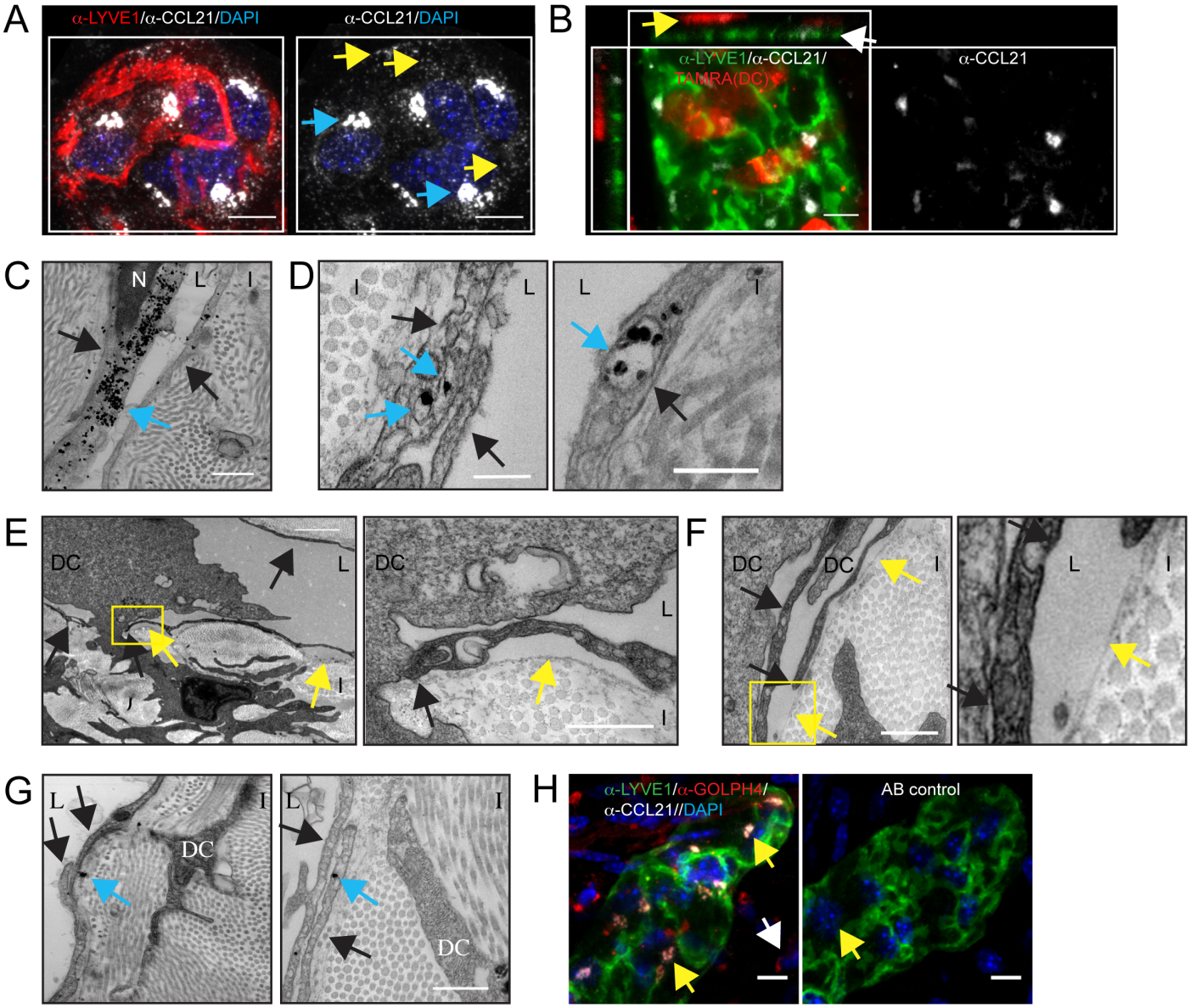
A
α-LYVE1/α-CCL21/DAPI
α-CCL21/DAPI
B
α-LYVE1/α-CCL21/
TAMRA(DC)
α-CCL21
C
N
L
I
D
I
L
L
I
E
DC
L
I
DC
L
I
F
DC
DC
I
L
I
G
L
I
DC
L
I
DC
H
α-LYVE1/α-GOLPH4/
α-CCL21//DAPI
AB control

Figure S1. CCL21 localization and DC-LEC interaction in dermal tissue. Related to Figure 1. (A) A blind end of mouse dermal lymphatic capillary stained for LYVE1 (red), CCL21 (white) and nucleus (DAPI, blue). Yellow arrows indicate some of the intracellular CCL21 vesicles and blue arrows Golgi deposits. **(B)** Staining of LYVE1 (green) and CCL21 (white) of the wild type dermis invaded by TAMRA labeled *Ccr7*$^{-/-}$ DCs (red). Yellow arrow depicts the DC and white arrow the lymphatic capillary in the orthogonal image. **(C-D and G)** Transmission electron micrographs of CCL21 staining of dermis. Black arrows indicate LECs and blue arrow silver-amplified CCL21 immunogold label, which are enriched (C) perinuclearly and (D) in vesicles, but (G) not enriched at the site of non-interacting DC and LEC. Interstitium (I), LEC nucleus (N), lumen (L) and DC are marked. **(E-F)** Transmission electron micrographs of LEC transmigrating DC. Black arrows indicate the LECs, yellow arrows the basement membrane at the site of detached LEC. Figures on the right show a zoom-in of the boxed region. Interstitium (I), lumen (L) and DC are marked. **(H)** On the left, a blind end of mouse dermal lymphatic capillary stained with anti-Lyve1 (green), anti-GOLPH4 (red), anti-CCL21 (white) and DAPI (nuclei, blue) and the appropriate secondary antibodies. On the right, an identical staining except the primary antibodies for GOLPH4 and CCL21 were omitted to control the specificity of the primary antibodies. Scale bars 10μm in (A-B), in (C) 500nm, in (D) 200nm, in (E) 2μm and 500nm in the inset, in (F) 500nm, in (G) 500nm and in (H) 10μm.

Figure S2

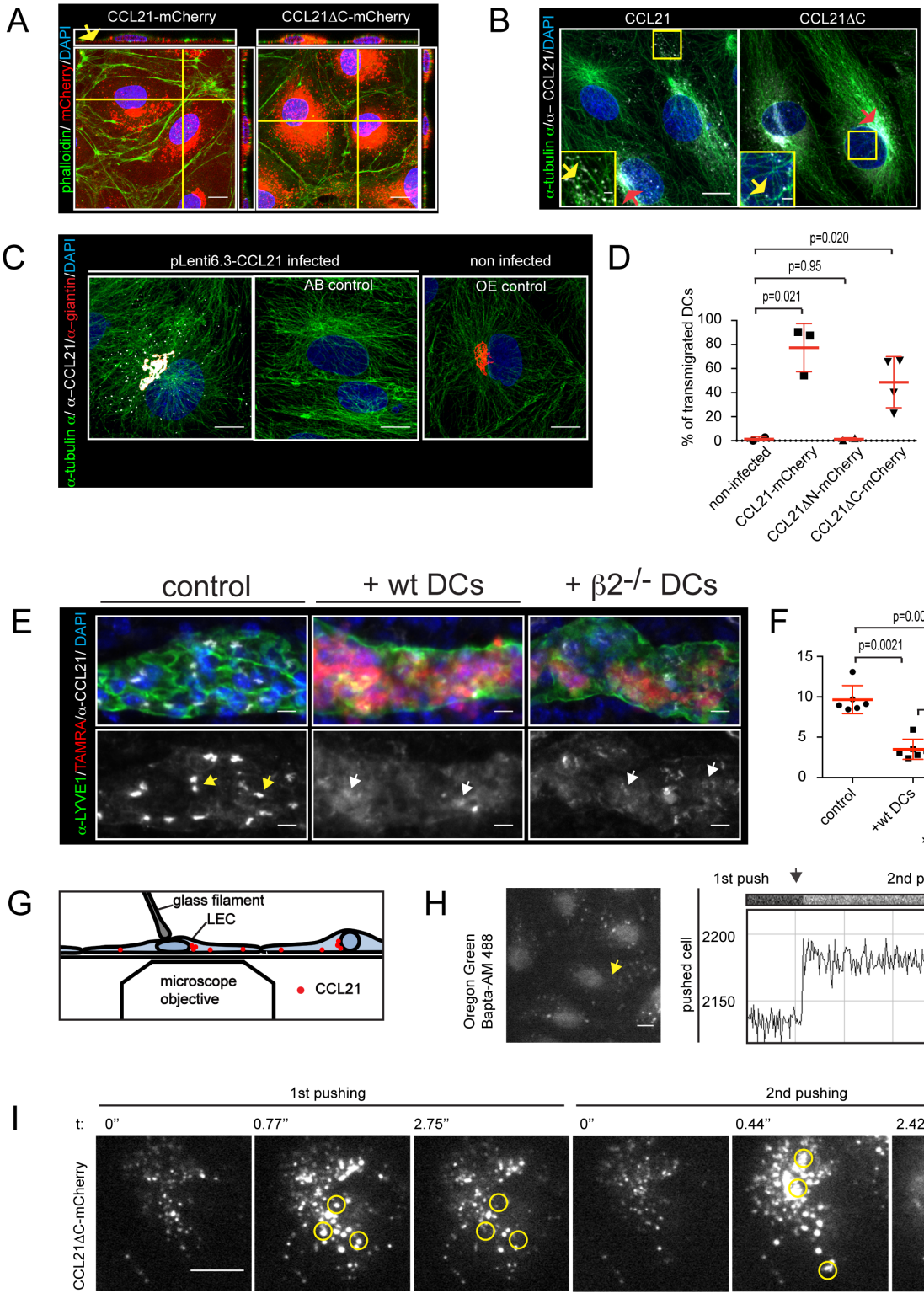
A
CCL21-mCherry
CCL21ΔC-mCherry
phalloidin/ mCherry/DAPI
B
CCL21
CCL21ΔC
α-tubulin α/α– CCL21/DAPI
C
pLenti6.3-CCL21 infected
non infected
AB control
OE control
α-tubulin α/ α–CCL21/α–giantin/DAPI
D
p=0.020
p=0.95
p=0.021
% of transmigrated DCs
100
80
60
40
20
0
non-infected
CCL21-mCherry
CCL21ΔN-mCherry
CCL21ΔC-mCherry
E
control
+ wt DCs
+ β2-/- DCs
α-LYVE1/TAMRA/α-CCL21/ DAPI
F
p=0.0012
p=0.0021
p=0.051
15
10
5
0
control
+wt DCs
+β2-/- DCs
G
glass filament
LEC
microscope objective
CCL21
H
Oregon Green Bapta-AM 488
1st push
2nd push
pushed cell
2200
2150
I
1st pushing
2nd pushing
t:
0”
0.77”
2.75”
0”
0.44”
2.42”
CCL21ΔC-mCherry

Figure S2. CCL21 localization in primary LEC cultures (related to figure 2), and effect of integrin β2$^{-/-}$ DC-LEC interaction in dermis or mechanical stimulus *in vitro* on CCL21 dispersion/secretion (related to figure 4). (A) Phalloidin (green) and DAPI (blue) staining of CCL21-mCherrry or CCL21ΔC-mCherrry (red) expressing LECs. Yellow lines indicate the plane of orthogonal sections and yellow arrow in the orthogonal section the extracellular CCL21-mCherry anchored on the cell culture dish surface. **(B)** Staining of tubulin-α (green), CCL21 (white) and nucleus (DAPI, blue) in LECs expressing non-tagged CCL21 or CCL21ΔC. Red arrows indicate the Golgi localized depots of CCL21 and yellow arrows in zoom-in boxes the MT associated CCL21. **(C)** Staining of tubulin-α (green), CCL21 (white), giantin (red) and nuclei (blue) in CCL21 overexpressing (OE) LECs (on the left) or non-infected LECs (on the right, OE control). Picture in the middle shows an antibody control, in which CCL21 and giantin primary antibodies were omitted. **(D)** Quantification of DC transmigration on non-infected, CCL21-mCherry, CCL21 ΔN-mCherry or CCL21 ΔC-mCherry expressing monolayers. For CCL21-mCherry and CCL21 ΔC-mCherry dot blot graph shows mean +/- SD of pooled samples from 3 independent experiments, n=3 or 4, respectively. Two of these independent experiments included non-infected or CCL21 ΔN-mCherry expressing monolayers for which n=2. Data is presented as percentage of transmigrated DCs. See video 4. **(E)** LYVE1 (green), CCL21 (white) and nuclei (DAPI, blue) of the ear dermis after 7h in presence or absence (control) of TAMRA labeled wild type or integrin β2$^{-/-}$ (β2$^{-/-}$) DCs (red). White arrows indicate dispersion of CCL21 (yellow arrow in control). **(F)** Dot blot graph shows ratio of signal in high intensity CCL21 depots to CCL21 in other areas of LECs. Columns represent mean values +/- SD of control (n=6), + wild type DC (n=6) or + integrin β2$^{-/-}$ (β2$^{-/-}$) DC (n=7) samples of approximately 300μm long lymphatic vessel stretches. **(G)** Schematic depicts experimental set up, in which the basolateral side of a LEC is imaged with TIRF microscopy while, due to limitations of the setup, the apical (luminal) side, instead of the physiological basolateral side, of the LEC is pushed by micromanipulator guided glass filament. **(H)** A still image of time-lapse imaged and 10μM Oregon Green BAPTA-AM (white) treated LEC monolayer. A kymograph and corresponding line graph of Oregon Green BAPTA-AM intensity shows the Ca fluxes for the cytoplasmic region of the pushed cell (yellow arrow). **(I)** Time-lapse imaging of 2 consecutive pushes of a single LEC in a monolayer expressing CCL21ΔC-mCherry (white). Pushing occurred at 2nd frames as seen by more intense mCherry signal. At 3rd frames many of the vesicles have been secreted. Some of the sites of vesicle secretion are highlighted prior and subsequent to the secretion with yellow circles. Scale bars are in (A-C, E, H-I) 10μm and 2μm in insets in (B).

Supplemental experimental procedures

Generation and labeling of bone marrow derived dendritic cells

For generation of mature DCs, bone marrow was extracted from femur and tibia of 8-12 weeks old C57BL/6J mice and cultured in R10 culture medium (RPMI1640 culture medium supplemented with 10% fetal calf serum, L-Glutamin and Penicillin/Streptomycin, all from Gibco) and GM-CSF hybridoma supernatant. Day 8 DCs were activated for 20h with 200ng/ml LPS (Sigma L2654). Activated DCs were labeled for 15' at room temperature with 6.7µM 5-(and-6-) carboxytetramethylrhodamine, succimidyl ester (TAMRA; molecular probes, Life Technologies) in phosphate buffered saline (PBS). The staining reaction was terminated by addition of R10 followed by centrifugation and resuspension of cells in R10. Prior to experimentation DCs were cultured for 1h at 37°C and 5% CO_2.

Ear sheet staining

For Fig. 1B-C, S1A and S2E fixed ear sheets were permeabilized with 0.15% Triton x-100 in PBS for 15', blocked with 1% bovine serum albumin (BSA, Sigma) in PBS for 1h and stained with anti mouse LYVE1 (R&D, MAB2125) and anti mouse CCL21 antibodies (R&D, BAF457) in the blocking buffer. For Fig. 1A and S1H ear sheets were permeabilized with 0.5% Triton x-100, blocked with 3% non-fat milk in 0.5% Triton x-100 in PBS for 1h and stained with anti mouse GOLPH4 (Abcam ab28049), LYVE1 (R&D, MAB2125) and CCL21 (R&D BAF457) antibodies diluted in blocking buffer. Fluorochrome conjugated secondary antibodies (α-rat Alexa fluor 488, Jackson Immunoresearch 712-546-150; α-rat Dylight 549, Jackson Immunoresearch 712-506-150; α-rabbit Cy3, Jackson immunoresearch, 111-165-144) and streptavidin (alexa fluor 647, Jackson Immunoresearch, 016-600-084) were diluted in 1% BSA in PBS. Finally, ear sheets were counter-stained with DAPI (Life Technologies, D1306). Imaging of ear sheets was carried out with a LSM700 upright microscope equipped with a Plan-Apochromat 20x water (numerical aperature 1.0) DIC objective and Zen 2011 software.

Transmission electron microscopy

For ultrastructural analysis (Fig. 4A and S1E-F), ears were fixed with half-Karnovsky's 2.5% glutaraldehyde (GA) and 2% PFA in 0.1M phosphate buffer (PB). Samples were treated with 2% osmium tetroxide in PB (40' at room temperature in the dark) and contrast enhanced by means in 1% uranyl acetate in 50% ethanol (30' at room temperature) and 2.6% lead nitrate in sodium citrate (5' at room temperature). Samples were then flat-embedded in epoxy resin (Durcupan® ACM) on greased glass slides. Regions of interest were dissected and re-embedded in epoxy resin. Serial ultrathin sections (70-80 nm) were cut with an ultramicrotome (Leica Microsystems UC7) and collected on formvar-coated copper slot grids.

For immunolocalization of proteins (Fig. 1E, 4B and S1C, D and G) a pre-embedding immunometal labeling technique (immunogold plus silver amplification) was applied. Ears were fixed with 4% PFA and 0.05% GA in PB for 25' at room temperature, permeabilized with 0.15% Triton x-100 and incubated in 50mM glycine in PBS for quenching of free aldehyde groups, followed by incubation in 1% BSA in PBS for blocking of nonspecific binding sites. Samples were immunostained with biotinylated anti CCL21 (R&D, BAF457) and nanogold®-streptavidin (Nanoprobes Inc.). Nanogold particles were amplified with silver using the HQ SilverTM Enhancement kit (Nanoprobes Inc.) for 6-8' at room temperature under light microscopy control. Samples were washed in MilliQ water and postfixed in 2% GA in PB prior to embedding in epoxy resin. Specificity of immunodetection was controlled and confirmed omitting primary antibodies with following application of the nanogold®-streptavidin. Ultrathin sections were cut at 80 nm and examined in a TECNAI 10 transmission electron microscope operated at 80 kV, equipped with a Morada CCD camera (Soft Imaging Systems). Alternatively, sections were cut at 250 nm, collected on formvar-coated 100-line bar grids, carbon coated (6 nm thickness) and observed under a Jeol JEM 2800 operated at 200 kV in STEM bright-field mode.

DNA constructs

For cloning of *Ccl21*, mouse spleen mRNAs were isolated (RNeasy mini kit, Qiagen) and converted to cDNA by reverse transcriptase reaction (Maxima H minus first strand cDNA synthesis kit, Thermo). Using cDNA pool as a template, *Ccl21* was amplified via PCR reaction (Phusion, Thermo scientific) with a 5'-cac ctc gag cat ggc tca gat gat gac tct g-3' forward and either with 5'- tga att cta tcc tct tga

ggg ctg tgt c -3' (with stop codon) or 5'- tga att cgc tcc tct tga ggg ctg tgt c -3' (without a stop codon) reverse primers followed by directional TOPO cloning (pENTR/D-TOPO, Invitrogen). To fuse *Ccl21* and mCherry, both pENTR/D-TOPO-Ccl21 and mCherry, which was amplified from pBabe-TetCMV-puro-mCherry-PA-Rac1 (Addgene, forward 5'-taagcagaattcaaagctggctagcatggtgag-3' and reverse 5'-tgcttagaattcttacttgtacagctcgtccatgcc-3' primers), were cut with EcoR1 and ligated with T4 ligase (Express link T4 ligase, Invitrogen) to yield pENTR/D-TOPO-Ccl21-mCherry. To delete the N- (amino acids 1-23) or C-terminus (amino acids 99-133) of the CCL21 we carried out a PCR based site directed mutagenesis (Phusion, Thermo scientific). For N-terminal deletion 5' phosphorylated 5'- agt gat gga ggg ggt cag gac tgc tgc ctt-3' forward and 5'- cat gct cga ggt gaa ggg ggc ggc c-3' reverse primers and for C-terminal deletion either 5'-gcg aat tca aag ctg gct agc atg gtg agc-3' (for pENTR/D-TOPO-Ccl21-mCherry) or 5'- tag aat tca aag ggt ggg cgc gcc-3' (for pENTR/D-TOPO-Ccl21-STOP) forward and 5'-ttt ccc tgg ggc tgg agg ctg gtc-3' reverse primers were used for amplification of a truncation mutant via PCR, which was followed by ligation. Finally, pLenti6.3-Ccl21-mCherry, pLenti6.3-Ccl21ΔC-mCherry, pLenti6.3-Ccl21ΔN-mCherry, pLenti6.3-Ccl21 and pLenti6.3-Ccl21ΔC were created by a LR-reaction (Invitrogen) between the pLenti6.3 (Invitrogen) and the above-described pENTR/D-TOPO vectors.

To obtain pLenti6.3-Lifeact-EGFP, attB1/2 gateway forward 5' ggg gac aag ttt gta caa aaa agc agg cta cca tgg gtg tcg cag att tga tc 3' and reverse 5' ggg gac cac ttt gta caa gaa agc tgg gtt tac ttg tac agc tcg tcc atg 3' primers were designed to amplify the DNA sequence via PCR from the plasmid described earlier (Riedl et al., 2008). The PCR product was then recombined into the pDONR221 donor vector (Invitrogen) via gateway BP reaction. The resulting plasmid was then used in a LR gateway reaction to obtain the plenti6.3 expression vector.

To obtain pLenti6.3-EGFP-tubulin α , EGFP-tubulin α 1B was amplified from EGFP-tubulin α 1B expression plasmid (a kind gift from professor Vic Small) with the attB1/2 gateway forward 5'-ggg gac aag ttt gta caa aaa agc agg ctt cac cat ggt gag caa ggg c -3' and reverse 5'- ggg gac cac ttt gta caa gaa agc tgg gtc gga tcc tta gta ttc ctc tcc ttc -3' primers. The PCR product was then recombined into the pDONR221 donor vector (Invitrogen) via gateway BP reaction. The resulting plasmid was then used in a LR gateway reaction to obtain the plenti6.3 expression vector.

Identification of putative nuclear localizing signal

cNLS mapper (http://nls-mapper.iab.keio.ac.jp/cgi-bin/NLS_Mapper_form.cgi) (Kosugi et al., 2009) was used to search the mature (the same as CCL21 ΔN) mouse CCL21 sequence for putative nuclear localization signal. A putative non-conserved bipartite nuclear localization signal covering aa's 21-50 was identified.

Virus production

Viruses encoding pLenti6.3-Ccl21, pLenti6.3-Ccl21ΔC, pLenti6.3-Ccl21-mCherry, pLenti6.3-Ccl21ΔC-mCherry, pLenti6.3-Ccl21ΔN–mCherry, pLenti6.3-Lifeact –EGFP and pLenti6.3-EGFP-tubulin α were produced in LentiX-293 packaging cells (Chemicon, Darmstadt, Germania) according to the protocols of Functional Genomics Unit of the University of Helsinki (http://www.helsinki.fi/fugu/).

LEC culture and infections

Primary human juvenile foreskin dermal lymphatic endothelial cells (LEC, C-12216, Promocell) were cultured in ready-to-use FCS and growth factor supplemented endothelial cell growth medium MV2 (Promocell, www.promocell.com, C-22022) in the absence of antibiotics. The LECs were checked for the expression of the CCL21 (R&D, MAB366) and podoplanin (Breiteneder-Geleff et al., 1999) (the antibody was a kind gift of Dontscho Kerjaschki). Small amounts of endogenous CCL21 were found confined in Golgi apparatus as reported earlier (Johnson and Jackson, 2010). Cells were used for experimentation at passages 4-6 and plated on 0.1% gelatin coated 1.5cm^2 large wells with #1.5 thick coverslip bottom or 24-well plates (day 0) and infected with 1:20 diluted viruses in the MV2 media in the presence of 9 μg/ml polyprene (Sigma) for 6-8h at day 1. The media was changed once/day and the cells were used for experimentation at day 3-5, 1 day subsequent to reaching full confluency.

Staining of LECs
The fixed samples were permeabilized with 0.15% Triton x-100 in PBS for 10', blocked with 1% BSA in PBS for 1h and stained with phalloidin (Alexa fluor 488, A12379 Thermo Fisher scientific) and anti human tubulin α (AbD Serotec, MCA77G), anti mouse CCL21 (biotinylated, R&D BAF457) and anti human giantin (Abcam ab24586) specific antibodies diluted in the blocking buffer. Fluorochrome conjugated secondary antibodies (α-rat alexa fluor 488, Jackson immunoresearch 712-546-150; α-rabbit alexa fluor 647, Jackson immunoresearch, 711-606-152) and streptavidin (alexa fluor 647, Jackson immunoresearch, 016-600-084) were diluted in 1% BSA in PBS. Finally, the LECs were counterstained with DAPI (Life Technologies, D1306). Stained cells were imaged with a Zeiss LSM700 inverted microscope equipped with a Plan-APOCHROMAT 63x/1.4 Oil objective and Zen 2011 software or with a LSM700 upright microscope equipped with Plan-Apochromat 20x water (numerical aperature 1.0) and 40x oil (numerical aperature 1.4) DIC objectives and Zen 2011 software.

Measurements of mCherry signals of the culture supernatant
The LEC culture supernatant was centrifuged at 500RCF for 6' and 200µl of the supernatant was transferred to black 96-well plates (Greiner). Fluorescence was measured with a Synergy H1 plate reader (Biotek, excitation 587nm and emission 620nm).

For the experiment shown in Fig. 2B, each of the cultures were stained with DAPI and imaged with Zeiss LSM700 inverted microscope equipped with Plan apochromat 20x dry (numerical aperature 0.8) objective and Zen 2011 software followed by quantification of infection efficiencies to normalize CCL21-mCherry and CCL21ΔC-mCherry levels relative to CCL21ΔN-mCherry. Finally, results were normalized to the background fluorescence of non-infected LEC culture supernatant, which was set as 1. Serial dilution of a 48h supernatant sample from CCL21ΔC -mCherry expressing LECs showed a linear increase in fluorescence upon increased amount of CCL21ΔC-mCherry supernatant.

Microscope setup for live TIRF imaging of CCL21-mCherry positive vesicles
Infected LECs were time-lapse imaged with an Olympus IX 83 microscope equipped with a Hamamatsu EMCCD C9100-13 camera, cell TIRF, UAPON 100X OTIRF objective (numerical aperature of 1.49), xcellence rt 2.0 software and an incubator with +37C and 5% CO_2 atmosphere.

Microscope setup for *In vitro* DC transmigration assay
Immediately after addition of DCs, phase contrast time-lapse imaging at 20'' frame frequency was started with a Leica DM IL LED microscope equipped with a S40/0.45 condensor, phase contrast, modulation and Leica HI PLAN CY 10x (numerical aperature 0.25) objective and an incubator with 37°C and 5% CO_2 atmosphere.

LEC Ca sensor assays
For the co-incubation of LECs and DCs, the TAMRA labeled DCs were washed twice with PBS after terminating the TAMRA reaction with RPMI1640 supplemented with 10% FCS, and resuspended in MV2 culture media (Promocell) supplemented with L-glutamin but devoid of growth factor supplement (Called hereafter MV2–). After preparing the DCs, the LECs were loaded either with fresh MV2– (control), MV2– DC conditioned supernatant, MV2– media with 100000 DCs or MV2– media with 100000 Mycalolide B (Santa Cruz), an irreversible actin depolymerizing agent (Hori et al., 1993; Saito et al., 1994), pre-treated 100000 DCs. The conditioned supernatant was produced by incubating 100000 DCs in MV2– media for 40' followed by centrifugation. Media with DCs was produced by adding 100000 DCs to MV2– media, which were co-incubated 20' prior to adding on the cells. Mycalolide B treated DCs were produced by incubating TAMRA labeled DCs in 1.0µM Mycalolide B for 15' followed by 3x washing with PBS and resuspension in MV2– media for 20' before loading on the LECs. The lack of actin dependent protrusion was confirmed with phase contrast microscopy.

Control, conditioned, DC containing or Mycalolide B pre-treated DC containing MV2– media (Promocell) was carefully added on a 1.5cm^2 well or Ibidi 8-well glass bottom µ-slide of day 4-5 confluent CCL21 overexpressing LEC monolayer, which had prior to loading been washed twice with MV2– media, treated for 50' with 10µM Oregon Green BAPTA-AM Ca sensor (Life Technologies, O6807) and washed twice with MV2– culture media. The time-lapse imaging was started 10' after loading the DCs at 2.2'' frame interval with a Nikon Eclipse Ti microscope equipped with Lumencolor

light engine, Hamamatsu ORCA R2 (model C10600) and EMCDD C9100-02 cameras, 10x PLAN FLUOR Ph1 DL (numerical aperature 0.3) and 20x PLAN FLUOR (numerical aperature 0.5) objectives, NIS-Elements AR 4.00.08 software and an incubator with 37°C and 5% CO_2 atmosphere. For the cell population analysis (Fig. 4E) imaging lasted for 10' and the number of LECs displaying transient Ca peaks was quantified from acquired videos.

Mechanical pushing of the cells

For mechanical pushing of the CCL21ΔC-mCherry expressing_LECs a glass pipette was heated and pulled into a thin filament. The tip of the glass filament was melted into a solid microsphere and then mounted on a micrometer driven x/y/z translation stage which itself was attached to the Olympus IX 83 microscope stage. In transmitted light the microsphere acted as lens which produced a bright focus which allowed for precise positioning of the microsphere above the nucleus of the cell of interest without touching the cell. Subsequently the microsphere was carefully lowered using the z-axis until a pushing force was applied to the cell. Concomitantly with pushing, the cells were time lapse imaged with_Olympus IX 83 microscope equipped with Hamamatsu EMCCD C9100-13 camera, cell TIRF, xcellence rt 2.0 software and an incubator with +37C and 5% CO^2 atmosphere. The TIRF mode and UAPON 100X OTIRF objective (numerical aperature of 1.49) were used to image the CCL21-mCherry secretion.

For monitoring of Ca fluxes upon mechanical pushing, the CCL21ΔC-mCherry expressing LECs were incubated with 10µM oregon green BAPTA-AM in supplemented MV2 culture media (Promocell, see cell culture) for 1h, washed twice with PBS and incubated with supplemented MV2 culture media (Promocell). The critical angle setting and UAPON 0340 40x objective (numerical aperature 1.15) were used to allow imaging of the whole oregon green BAPTA-AM treated LECs in Z-direction. The Ca sensor intensity (oregon green BAPTA-AM) kymographs were created and analyzed with FiJi software.

Image analysis

CCL21-mCherry vesicles were tracked automatically using ImarisTrack (Imaris 7.4, BITPLANE). The resulting tracks were filtered by track length and track displacement and then manually classified and color-coded accordingly (see Fig. 2C).

To quantify the dispersion of LEC intracellular CCL21 upon DC transmigration (Fig. 1C-D and S2E-F), 300µm long stretches of lymphatic capillary in confocal images were presegmented using Ilastik (ilastik.org) and cleaned up manually. The resulting binary images were eroded to avoid edge effects and converted into masks. Likewise perinuclear CCL21 regions were segmented employing intensity based thresholding and converted into masks. Using Fiji a representative background region was drawn manually and the raw CCL21 intensities of the background (non-specific staining, detection offset)(I_B), perinuclear region (I_PN) and rest of LV (I_LV) were measured. The enrichment in the perinuclear region is then given by: (I_PN-I_B)/(I_LV-I_B).

Fiji software was also used for brightness/contrast adjustment of images and videos and for length measurements of LECs in transmission electron micrographs.

References

Breiteneder-Geleff, S., Soleiman, A., Kowalski, H., Horvat, R., Amann, G., Kriehuber, E., Diem, K., Weninger, W., Tschachler, E., Alitalo, K., et al. (1999). Angiosarcomas Express Mixed Endothelial Phenotypes of Blood and Lymphatic Capillaries. The American Journal of Pathology *154*, 385–394.

Hori, M., Saito, S.-Y., Shin, Y.Z., Ozaki, H., Fusetani, N., and Karaki, H. (1993). Mycalolide-B, a novel and specific inhibitor of actomyosin ATPase isolated from marine sponge. FEBS Letters *322*, 151–154.

Johnson, L.A., and Jackson, D.G. (2010). Inflammation-induced secretion of CCL21 in lymphatic endothelium is a key regulator of integrin-mediated dendritic cell transmigration. International Immunology *22*, 839–849.

Kosugi, S., Hasebe, M., Tomita, M., and Yanagawa, H. (2009). Systematic identification of cell cycle-dependentyeast nucleocytoplasmic shuttling proteinsby prediction of composite motifs. Proceedings of the National Academy of Sciences *106*, 10171–10176.

Riedl, J., Crevenna, A.H., Kessenbrock, K., Yu, J.H., Neukirchen, D., Bista, M., Bradke, F., Jenne, D., Holak, T.A., Werb, Z., et al. (2008). Lifeact: a versatile marker to visualize F-actin. Nat Meth *5*, 605–607.

Saito, S.-Y., Watabe, S., Hiroshi, O., Fusetani, N., and Karaki, H. (1994). Mycalolide B, a Novel Actin Depolymerizing Agent*. The Journal of Biological Chemistry *269*, 29710–29714.